Pyrolysis of Large Black Liquor Droplets

Tadas P. Bartkus [a] Daniel L. Dietrich [b,*], James S. T'ien [a]
Richard A. Wessel [c]

[a] *Department of Mechanical and Aerospace Engineering, Case Western Reserve University; 10900 Euclid Ave., Cleveland, Ohio 44106, USA*

[b] *NASA John H. Glenn Research Center; 21000 Brookpark Rd., Mail Stop 110-3, Cleveland, Ohio 44135, USA*

[c] *The Babcock & Wilcox Company; 20 S. Van Buren Ave., Barberton, Ohio 44203, USA*

Abstract

This paper presents the results of experiments involving the pyrolysis of large black liquor droplets in the NASA KC-135 reduced gravity aircraft. The reduced gravity environment facilitated the study of droplets up to 9 mm in diameter extending the results of previous studies to droplet sizes that are similar to those encountered in recovery boilers. Single black liquor droplets were rapidly inserted into a 923 K oven. The primary independent variables were the initial droplet diameter (0.5 mm to 9 mm), the black liquor solids content (66.12% - 72.9% by mass), and the ambient oxygen mole fraction (0.0 - 0.21). Video records of the experiments provided size and shape of the droplets as a function of time. The results show that the particle diameter at the end of the drying stage (D_{DRY}) increases linearly with the initial particle diameter (D_O). The results further show that the ratio of the maximum swollen diameter (D_{MAX}) to D_O decreases with increasing D_O for droplets with D_O less than 4 mm. This ratio was independent of D_O for droplets with D_O greater than 4 mm. The particle is most spherical at the end of drying, and least spherical at maximum swollen size, regardless of initial sphericity and droplet size.

Key words: Black Liquor, Drying, Devolatilization, Pyrolysis, Combustion, Sphericity, Reduced Gravity
PACS: 82.30.Lp, 82.33.Vx

* Corresponding author.
  Email addresses: `tadas.bartkus@case.edu` (Tadas P. Bartkus), `Daniel.L.Dietrich@nasa.gov` (Daniel L. Dietrich), `jst2@mae.cwru.edu` (James S. T'ien), `rawessel@babcock.com` (Richard A. Wessel).

1 Introduction

Black liquor is the major by-product of the kraft process for the production of pulp [1] and one of the most important industrial fuels. A weak solution of black liquor (15 percent solids mass in water) is what results when the lignin in wood chips dissolves in a solution of sodium hydroxide and sodium sulfide. The actual black liquor fuel contains 65 to 85 percent solids in mass and is very thick and viscous after some of the water evaporates from the weak solution. Tomlinson recovery boilers burn black liquor for the purpose of energy production (approximately 1 percent of the total annual energy production in the United States) and chemical recovery of the inorganic salts [1]. During combustion, the fuel is injected into the boiler as a spray of droplets, where the typical droplet sizes range between 0.5 and 6 mm in diameter [2].

Previous studies [3,4,5,6] established that black liquor combustion occurs in four main stages: drying, devolatilization, char burning, and smelt oxidation. The first two stages comprise the pyrolysis of a black liquor droplet. Figure 1 shows these four stages with the particle (droplet) diameter as a function of time for an initially room temperature black liquor droplet rapidly inserted into a 923 K oven. The four stages are not strictly consecutive, as the physical processes overlap significantly during combustion due to large radial gradients in temperature and composition within the droplet. The precise definition of each stage varies in the literature because of the overlap between the stages, but in general they are as follows.

The drying period is the time period from insertion of the particle into the furnace to the time just prior to rapid expansion of the droplet. During the drying stage, the droplet undergoes violent disruptions, from the evaporation of water and decomposition of organic matter within the droplet. These rapid changes in droplet diameter are clear evidence of the disruptions during the drying stage. Previous tests with small black liquor droplets have shown that during the drying period, a single droplet typically swells between 1.3 to 1.8 times its initial diameter [4,7].

The devolatilization stage is the period from initial rapid expansion of the droplet to the time when it reaches the maximum swollen volume. During this period, the droplet increases continuously in size along with the particle internal temperature. As the internal droplet temperatures reach approximately 473 K , the organic material in the black liquor decomposes releasing gas-phase volatiles, which include CO_2, CO, H_2, other light hydrocarbons, H_2S, NO, and NH_3. If the temperature and oxygen mole fraction of the gaseous environment are high enough (above 823 K and 0.10, respectively), the released volatiles ignite and form a gaseous flame close to the droplet [8].

The third stage of black liquor droplet combustion is char burning and it is the longest stage. This stage is the time period from maximum swollen volume to the formation of a smelt bead. At the start of char burning the particle contains only carbon and inorganic salts. The carbon reacts with oxygen at the surface of the particle to form CO and CO_2. The carbon also reacts with CO_2 and H_2O to form CO and H_2, known as gasification, and reacts with inorganic salts, particularly Na_2SO_4 (sodium sulfate) to form Na_2S (sodium sulfide). The particle shrinks in size during this stage until it becomes a smelt bead containing primarily inorganic salts [8].

Smelt oxidation is the fourth stage and is defined as the time period from the formation of a smelt bead to visible cooling of the bead [9]. During this stage the inorganic smelt bead undergoes reactions with the surrounding gases. Sodium sulfide (Na_2S) is oxidized to sodium sulfate (Na_2SO_4) [8].

Previous studies of black liquor combustion used experimental hardware designed to simulate conditions that occur with recovery boilers. Typical experimental configurations were of a fiber-supported droplet rapidly inserted into a quiescent, heated gas [6], a fiber-supported droplet rapidly inserted into an upwardly flowing, heated gas [4], or a droplet injected into a co-flowing, heated gas [5]. The times and particle diameters discussed above typically come from video or photographic records of the experiment. While the ambient conditions and fuels were typical of that in recovery boilers, the diameters of the droplets employed were in the smaller range of actual applications. Large droplets tend to fall off the support fibers when heated in the fiber-supported tests or require unreasonably long reactors in the injected droplet tests.

The current study extends the work available in the literature to larger droplet sizes, up to and even greater than those typically observed in recovery boilers. The experimental configuration is that of a fiber-supported droplet quickly inserted into a quiescent, heated ambient in a small furnace in reduced gravity. The reduced-gravity environment was achieved aboard the NASA KC-135 aircraft. Reduced gravity eliminates the problem of the droplet falling off of the support fiber.

2   Materials and Methods

By flying a particular parabolic trajectory, the NASA KC-135 reduced gravity aircraft can produce a reduced gravity condition (on the order of 10^{-2} earth gravity) nominally for 20-25 seconds [10,11]. Figure 2 shows a schematic of the experimental hardware. The apparatus consisted of a 26 *liter* pressure chamber inside of which was a small, cylindrical, high temperature, ceramic oven (inside oven dimensions: 89 *mm* diameter, 92 *mm* length). The oven

temperature was approximately 923 K ($\pm$ 5 K) for all of the tests. The oven and pressure chamber had orthogonal windows to enable video imaging of the droplet and flame. The droplet support was a horizontal wire of either a type K thermocouple (0.127 mm diameter) or aluminum alloy wire (0.279 mm diameter). For some tests, a second wire (0.279 mm diameter aluminum alloy), orthogonal to the first wire stabilized the droplets. These wire(s) supported droplets 0.5 mm to 9.0 mm in diameter outside the oven before entering reduced gravity. The oven quickly moved (in approximately 0.1 seconds) over the wire-supported droplet after the experiment package entered reduced gravity. As the droplet entered through an 8.9 cm by 1.5 cm slot at the bottom of the oven, an inherent flow was induced around the droplet from the oven movement. Quantitative convection effects from this motion were not measured, but are assumed to be small as flows dissipated relatively quickly.

The primary independent variables were the initial droplet diameter, black liquor solids content, and ambient oxygen mole fraction. Three black liquor fuel samples of varying solids content were supplied by The Babcock & Wilcox Company (actual samples taken from a recovery boiler). The three fuels had solids mass concentrations of 66.12 percent (Fuel 1), 67.53 percent (Fuel 2) and 72.9 percent (Fuel 3). The oxygen mole fraction varied between 0.00 and 0.21 (balance nitrogen). These oxygen mole fraction values are typical for black liquor recovery boilers.

The data from the experiment were from orthogonal video views of the burning history, one with a backlight and the other with indirect illumination and/or natural flame luminosity of the droplet. The video data yielded the particle size, shape and estimates of four times described in the previous section. As the droplet expanded during the devolatilization stage, it became too big for the small field of view in the backlit camera. Therefore the majority of the data came from the video camera with indirect illumination and/or natural flame luminosity (flame-view).

Figure 3 shows a typical flame-view image sequence of a black liquor particle during a pyrolysis test. Figure 3 depicts the droplet (a) as it enters the oven denoting the start of the drying stage; (b) during the drying stage; (c) at the start of the rapid expansion; and (d) at maximum swollen size.

The particle diameter reported in this article is an equivalent diameter. There are at least two reasons that a droplet is not entirely spherical. The first is due to gravity (the droplet frequently became distorted during the $2 - g$ pull up before entering reduced gravity). The second is due to the high viscosity of the black liquor fuel caused by the high solid content. The traditional techniques used to automatically measure the diameter of pure liquid droplets [12] were not effective because of the difficulty in discerning the edge of the black liquor droplet and the lack of contrast between the droplet and background. Thus,

the approach in this work was less automated. After transferring the video data to a microcomputer, the particle was manually outlined in each frame of interest. The computer then counted the pixels inside this outline (boundary) to determine the projected area (A_P). The equivalent diameter (D_{AP}) is the diameter of a sphere with the same projected area as that measured (Eq. 1).

$$D_{AP} = \sqrt{\frac{4A_P}{\pi}} \tag{1}$$

To estimate the uncertainty in the particle diameter data, we assume that the particle boundary was 1 pixel beyond that manually traced. In reality, this procedure overestimates the error since this outline is clearly outside the edge of the droplet. For small droplets, the change in D_{AP} was relatively large (approximately 18% for a 1 mm particle). For large droplets, however, the error decreases considerably (approximately 3% for a 6 mm particle). The time resolution is that of a single video frame, or 33 ms.

The sphericity factor (S_1) is the ratio of the circumference (C_d) of a circle with diameter D_{AP}, to the circumference (C) measured from the manual outline of the particle (Eq. 2). This factor is a measure of how far the particle deviates from a sphere (or a circle in terms of a two dimensional measurement). A perfect sphere (or circle) has $S_1 = 1$, while on the other extreme, an infinitely long line has $S_1 = 0$. As a point of reference, ellipses with major axis to minor axis ratios of 2/1 and 3/1 have values of $S_1 = 0.92$ and $S_1 = 0.81$, respectively. Calculating the particle sphericity for black liquor combustion is important since heat transfer rate is directly related to surface area.

$$S_1 = \frac{C_d}{C} = \frac{\pi D_{AP}}{C} \tag{2}$$

3   Results and Discussion

This work examined initial droplet sizes between 0.5 and 9.0 mm. The tests with smaller droplet sizes facilitate comparison with existing studies. The tests with the larger droplets, with sizes similar to those in recovery boilers, represent the unique contributions of this work. Some of the small droplet tests occurred in normal gravity. All of the large droplet tests, however, required the reduced gravity environment of the aircraft. There was some overlap in the droplet sizes tested in normal and reduced gravity to assess the gravity dependence of the results.

While the reduced gravity environment enabled the suspension of large black liquor droplets on fibers, the test time is limited to approximately 25 sec-

onds. This was insufficient time to observe the entire pyrolysis (drying and devolatilization), ignition and combustion process for large droplets. Therefore, the emphasis of this work is on the drying and devolatilization stages, which could be completely observed in the available test time.

In the first two stages, the dominant physical processes are heat and mass transfer between the droplet and the ambient and not chemical kinetics. As a result, one would expect and in fact, the data show, that changes in ambient oxygen mole fraction do not significantly influence the drying and devolatilization times. Therefore, we present the data for drying and devolatilization without differentiating between the different ambient oxygen mole fractions. Any influence due to the ambient oxygen mole fraction is within the scatter of the data.

Similarly, the data for drying and devolatilization were found to be independent of gravity level for the smaller particle sizes. The primary purpose of performing the experiments in reduced gravity was therefore to be able to observe the behavior of large black liquor droplets. The reduction or elimination of buoyancy-induced flows did not significantly affect the drying and devolatilization behavior of smaller droplets. Therefore, we present the data without any differentiation between gravity levels, since the variations due to gravity level are much less than the scatter in the data.

3.1   Drying Stage

Figure 4a shows the diameter of the droplet at the end of the drying period (D_{DRY}) versus initial droplet diameter (D_O). According to Figure 4a, D_{DRY} increases linearly with increasing initial diameter for all three fuels. Figure 4b shows the ratio $\frac{D_{DRY}}{D_O}$, or the drying ratio, versus initial droplet diameter. According to Figure 4b, the drying ratio varies between 1.2 and 1.8 over the entire range of D_O with an average of about 1.5 for all fuels and initial droplet diameters. For the range of $D_O < 2.3\,mm$, the present results are consistent with data in previous small droplets experiments [7].

Figures 4a and 4b further show that the drying ratio is independent of solids content in the black liquor. Figure 4b does show that the scatter in drying ratio data is more prominent with Fuels 1 and 2, while Fuel 3 maintains a slightly smaller band of scatter. The average drying ratio, however, is about 1.5 for all three fuels and therefore independent of solids content. This is in agreement with Miller [13], who observed for small black liquor droplets that the drying ratio is independent of solids content between 60% and 85% solids mass content.

Figure 4c shows the drying time (T_{DRY}) as a function of initial particle diame-

ter. The drying time increases rather rapidly with increasing initial droplet diameters between 0.5 and 2 mm. At larger initial droplet sizes, the present data show that this dependence decreases with increasing D_O, and the scatter in the data increases. This decrease in slope may be the result of in-homogeneous heating and drying within the droplet. A large droplet, while drying, may become dry at the surface and at this point begin expanding (representing the end of drying). The interior of the droplet, however, is still not completely dry. The early exit from the drying stage (or entry into the devolatilization stage) and the scatter in the data may indicate that heat and mass transfer within the droplet, which are not significant for smaller initial droplet sizes, become more important and even dominant for larger sizes. For the range of $D_O < 2\,mm$, the present results are consistent with the small droplet data in previous experiments [5].

The scatter in the data in Fig. 4c emphasizes the somewhat ambiguous definition for the drying stage (and consequently, the devolatilization stage) and the difficulty in discerning the end of the drying stage for large black liquor droplets. The black liquor combustion stages are not necessarily discrete and consecutive. In this and previous studies, the stages are treated as discrete and sequential, when in actuality overlap may exist. The present data suggest that this overlap in stages between drying and devolatilization may be more prominent with larger droplets with larger radial temperature and moisture gradients within the droplet.

Finally, the data in Fig. 4c show that the drying time is relatively independent of fuel solids content for droplets with initial sizes greater than 2 mm. Only tests with Fuel 3 (the highest solids content) provide substantial data on drying times for initial diameters greater than 6 mm.

3.2   Devolatilization Stage

Figure 5a shows the ratio of the maximum droplet diameter (D_{MAX}) to the initial droplet diameter (D_O). The largest value of $\frac{D_{MAX}}{D_O}$ for all three fuels is approximately 6, at values of D_O between 1.0 and 1.5 mm. The scatter in $\frac{D_{MAX}}{D_O}$ data is very large for initial diameters less than 1.5 mm. At initial droplet diameters greater than 1.5 mm, $\frac{D_{MAX}}{D_O}$ begins to gradually decrease reaching a value between 2 and 3 at a D_O of 4 mm. The scatter in the data also decreases in this range. At initial droplet diameters greater than 4 mm, $\frac{D_{MAX}}{D_O}$ for all three fuels levels remains nearly constant at 2.75 ± 0.25. The decrease in $\frac{D_{MAX}}{D_O}$ with increasing D_O may be attributed to changes in heating rate. Large droplets heat up more slowly and have larger internal radial gradients than small droplets. These larger droplets therefore have a lower rate of volatile gas release per unit volume. As a result of this lower gas release rate, large

droplets allow for more time for gas to escape and have less tendency to swell. All three fuels have similar trends, and have very similar values for $\frac{D_{MAX}}{D_O}$ for the entire range of initial diameters. A similar conclusion on the independence on fuel solid content has been reported [13] based on small droplet data.

Figure 5b shows how the devolatilization time, T_{DEV}, is dependent on initial diameter for all three fuels. This study extends the relationship between T_{DEV} and D_O for initial droplet diameters greater than 2 mm. Devolatilization time increases nearly linearly for all three fuels for values of D_O ranging from 0.5 mm to over 9 mm. According to Figure 5b the ratio of devolatilization time to initial droplet diameter is approximately 1.25 s/mm. Figure 5b shows that the scatter in devolatilization time increases as initial diameter increases. Similar to the argument described in the drying results section, this increase in data scatter for T_{DEV} with respect to increasing D_O may be the result of treating the stages as discrete and consecutive. There is likely overlap between the drying and devolatilization which becomes more prominent with larger droplets, resulting in a larger scatter in the data. Figure 5b shows devolatilization times of about 2.0 s for droplets with initial diameters of 1.5 mm. This is comparable with results from Noopila and Hupa [14] where devolatilization times ranged from 1.1 to 2.3 s for tests performed in air at 973 K with droplets 2.2 mm in initial diameter.

3.3 Sphericity Results

Table 1 tabulates the sphericity at each stage for four test groups where only the oxygen mole fraction varies within each group. With the exception of changes in ambient oxygen mole fraction all of the tests in each group have the same test conditions. Table 1 shows the droplet sphericity at the beginning of the test (S_O), at the end of the drying stage (S_{DRY}), at the maximum swollen volume (S_{MAX}), and depending on the type of test conducted, at the end of the char burning stage (S_{CHAR}), or at the end of the shrinking stage (S_{SHRINK}). Droplet shrinking (not related to char burning) was observed in very low oxygen mole fraction tests.

Table 1a tabulates sphericity for tests run with Fuel 1 in normal gravity for droplets with an initial droplet diameter of 1.51 mm ($\pm$ 0.09 mm). Table 1b is sphericity data for tests conducted with Fuel 1 in reduced gravity for droplets with an initial droplet diameter of 2.83 mm ($\pm$ 0.14 mm). Table 1c represents tests conducted with Fuel 3 in normal gravity for droplets with an initial droplet diameter of 4.41 mm ($\pm$ 0.19 mm). Table 1d tabulates sphericity data for Fuel 2 in reduced gravity for droplets with an initial droplet diameter of 4.69 mm ($\pm$ 0.18 mm).

For tests conducted in normal gravity (Tables 1a and 1c), the droplets are initially quite spherical, where most S_O values are close to unity. Most of the initial sphericity values for tests conducted in reduced gravity (Tables 1b and 1d) are significantly lower than the normal gravity tests with S_O ranging from 0.71 to 0.96. Low S_O values occurred because droplets were deployed on the thin support wire during a high gravitational period of the airplane maneuver ($\approx$ 1.8 times normal gravity), which created deformed, elongated initial droplets (note, however, the droplet did not fall off the supporting wire because it was at a low temperature before the droplet entered the oven).

Irrespective of S_O, the S_{DRY} value is approximately 0.9 for all tests in each of the four groups. This result suggests that the shape of the droplet at the end of drying is fairly spherical and is relatively independent of initial droplet size, gravity condition, oxygen content, fuel solids content (for solids mass percentages between 66.12% and 72.9%) and initial sphericity. The increase in sphericity by the end of drying for particles with low S_O may be attributed to a change in viscosity. As particle temperature increases, viscosity decreases, and surface tension pulls the droplet together to form a near spherical shape by the end of drying. At the same time, vaporized water and volatiles escaping from the droplet distorts the shape and keeps it from being highly spherical by the end of drying.

As the droplet progresses from the end of the drying stage the sphericity decreases and reaches its lowest value at droplet maximum size. This decrease in sphericity by the end of devolatilization is due to the rapid release of volatile gases combined with the loss of droplet elasticity (the particle is devoid of water and contains only carbon and inorganic salts). These two attributes result in a random expansion that is not very spherical. Previously, Clay et al. [4] reported that shape irregularity increases as the droplet reaches advanced stages but no quantitative measurement had been made.

Table 1 shows that S_{MAX} generally decreases as the ambient oxygen mole fraction increases. Significant exothermic reaction of the volatile gases (combustion) did not impact these S_{MAX} results since gas phase combustion occurred only after maximum swollen volume was reached. The affects of initial droplet diameter, gravity type and fuel solids content (for solids mass percentages between 66.12% and 72.9%) on S_{MAX} were not discernible from the scatter in data.

As the droplet progresses from the end of devolatilization to the end of char burning, the sphericity increases significantly for the complete combustion test. A high sphericity value is expected since the charring particle collapses into a small bead, which is rather spherical. Partial combustion occurred for test conditions where oxygen content was sufficient to ignite the volatiles, but not burn the char to a small bead. In the cases in which partial combus-

tion occurred the sphericity remains approximately constant from S_{MAX} to S_{CHAR}. Similarly, in the purely pyrolysis tests (no combustion of any kind), the sphericity remains relatively constant from S_{MAX} to S_{SHRINK}. Any influence of initial diameter, gravity condition and fuel solids content (for solids mass percentages between 66.12% and 72.9%) on S_{CHAR} and S_{SHRINK} are again difficult to discern from the scatter in the data.

4   Summary and Conclusions

The study presented experimental results from approximately 50 normal gravity and 50 reduced gravity black liquor combustion tests. The reduced gravity experiments provided data on droplets between 2 and 9 mm that are very difficult to study in normal gravity because of experimental limitations. The normal gravity tests provided data on smaller initial droplet sizes, from 0.5 to 4 mm. The reduced gravity tests extend previous data dependent on and related to initial diameter, which was previously limited to droplet sizes less than 2.7 mm, and relates more closely to the initial droplet diameter that is typically found in a recovery boiler, 0.5 to 6 mm. This work focused primarily on the pyrolysis of black liquor which involves the drying and devolatilization stages. The specific conclusions of the study are:

(1) The particle diameter at the end of drying (D_{DRY}) increases linearly with increasing initial droplet diameter (D_O) over the entire range of initial droplet diameters studied. The ratio of D_{DRY} to D_O is 1.5 for initial droplet diameters ranging from 0.5 to 9 mm.

(2) The ratio of maximum particle diameter (D_{MAX}) to initial droplet diameter reaches its highest value at small initial droplet diameters, and decreases with increasing D_O. This ratio decreases until it levels off to a constant value of 2.75 ± 0.25 for initial diameters greater than 4 mm.

(3) The drying time (T_{DRY}) increases with increasing D_O, but increases at a slower rate for large initial diameters. The devolatilization time (T_{DEV}) increases fairly linearly with increasing D_O. The scatter for both drying time and devolatilization time increases as initial diameter increases.

(4) The finer affects of gravity level, fuel solids content (for solids mass percentages between 66.12% and 72.9%), and oxygen content on the swelling and time duration for drying and devolatilization typically could not be distinguished from the scatter in the data.

(5) The shape of the droplet at the end of drying is fairly spherical and is relatively independent of initial droplet size, gravity condition, oxygen content, fuel solids content (for solids mass percentages between 66.12% and 72.9%) and initial sphericity. A sphericity value of approximately 0.90 is measured for all droplets at the end of the drying stage.

(6) The droplet sphericity reaches its lowest value at maximum swollen droplet

diameter and is lowest with high oxygen content. The affects of initial droplet diameter, gravity type and fuel solids content (for solids mass percentages between 66.12% and 72.9%) on the sphericity of the particle at maximum swollen size (S_{MAX}) could not be distinguished from the scatter in the data.

References

[1] A. Maček, Research on combustion of black-liquor drops, Progress in Energy and Combustion Science 25 (1999) 275–304.

[2] A. Kankkunnen, P. Miikulainen, M. J. M., The ratio of ligaments and droplets of black liquor sprays, in: International Chemical Recovery Conference, Whistler, British Columbia, Canada, 2001, pp. 51–54.

[3] D. T. Clay, T. M. Grace, R. J. Kapheim, H. G. Semerijian, A. Maček, S. R. Charagundla, Fundamental studies of black liquor combustion, Report No. 1-Phase 1 DE85013773, US Department of Energy (1985).

[4] D. T. Clay, T. M. Grace, R. J. Kapheim, H. G. Semerijian, A. Maček, S. R. Charagundla, Fundamental studies of black liquor combustion, Report No. 2-Phase 1 DE88005756, US Department of Energy (1987).

[5] D. T. Clay, S. J. Lien, T. M. Grace, H. G. Semerijian, A. Maček, N. D. Amin, Fundamental studies of black liquor combustion, Report No. 2 - Phase 1 DE-AC02-83CE40637, US Department of Energy (1989).

[6] M. Hupa, P. Solin, P. Hyoty, Combustion behavior of black liquor droplets, Journal of Pulp and Paper Science 13 (2) (1987) J67–J72.

[7] W. J. Frederick, T. Noopila, M. Hupa, Swelling of spent pulping liquor droplets during combustion, Journal of Pulp and Paper Science 17 (5) (1991) J164–J170.

[8] T. N. Adams, W. J. Frederick, T. M. Grace, M. H. K. Iisa, A. K. Jones, Kraft recovery boilers, TAPPI Press, Norcross, Georgia, 1997.

[9] C. L. Verrill, Inorganic aerosol formation during black liquor drop combustion, Ph.D. thesis, Institute of Paper Science and Technology, Atlanta, Georgia (1994).

[10] H. D. Ross, Basics of microgravity combustion, in: H. D. Ross (Ed.), Microgravity Combustion: Fire in Free Fall, Combustion Treatise, Academic Press, 2001, Ch. 1, pp. 1–34.

[11] K. Schubert, NASA reduced gravity research program, http://exploration.grc.nasa.gov/ground/aircraft.html (2005).

[12] P. M. Struk, M. Ackerman, V. Nayagam, D. L. Dietrich, On calculating burning rates during fiber supported droplet combustion, Microgravity Science and Technology XI/4 (1998) 144–151.

[13] P. T. Miller, Swelling of kraft black liquor. an understanding of the associated phenomena during pyrolysis., Ph.D. thesis, The Institute of Paper Chemistry, Appleton, Wisconsin (1986).

[14] T. Noopila, Measuring the combustion properties of black liquors by different techniques, Tech. Rep. 88-5, Combustion Chemistry Research Group, Åbo Akademi, Turku, Finland (1988).

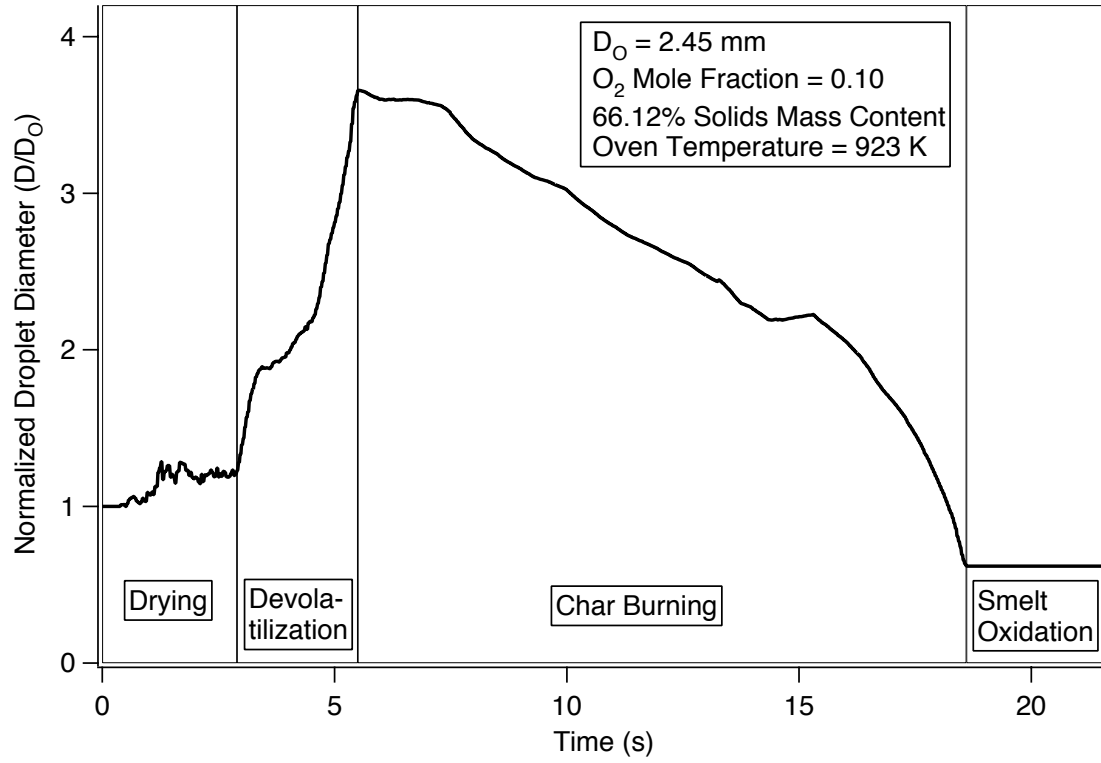**List of Figures**

13

List of Tables

Fig. 1. Droplet diameter history a 2.45 mm black liquor droplet undergoing combustion in an oven at 923 K and oxygen mole fraction of 0.10. The droplet combustion process is characterized by four stages: drying, devolatilization, char burning, and smelt oxidation
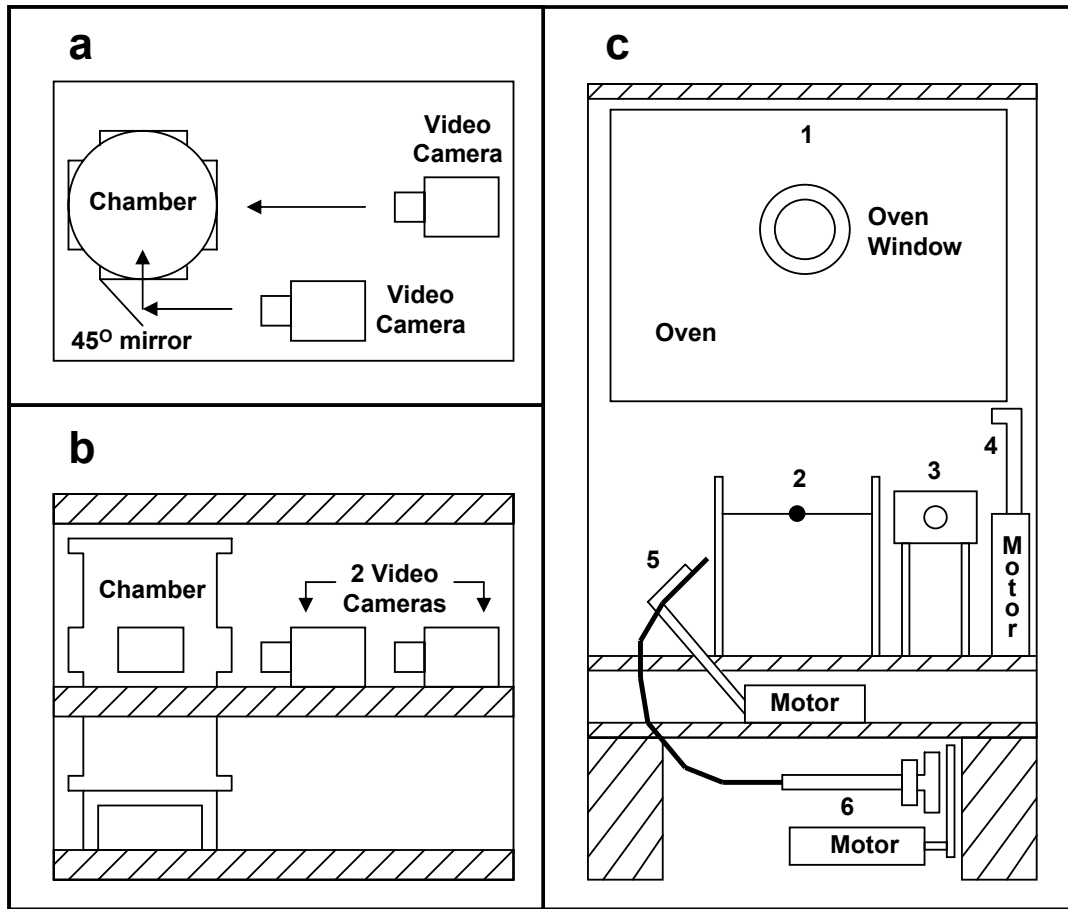
Fig. 2. Schematic drawings of the experimental apparatus (a) from the top (b) from the side and (c) the oven assembly located inside of the chamber. Orthogonal video cameras (shown in (a) and (b)) record droplet activity within the pressure chamber. Numbers in (c) denote the individual components of the oven assembly. Number 1 is the oven, 2 is a droplet of black liquor suspended from a thin wire, 3 is a light emitting diode (LED) used as a back light, 4 is an oven release motor, 5 is a movable mechanical arm and 6 is a syringe filled with black liquor.
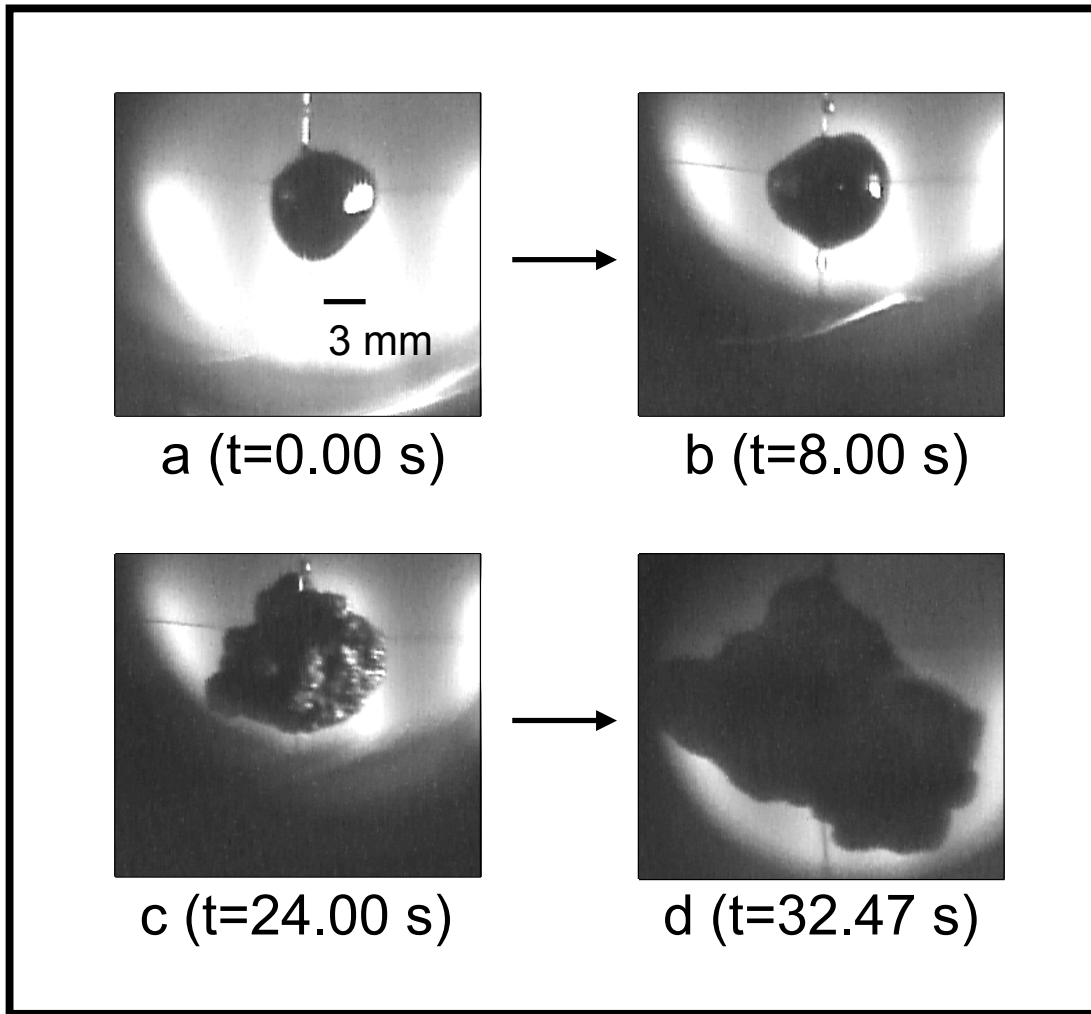
Fig. 3. An image sequence of a black liquor droplet undergoing pyrolysis in reduced gravity. The droplet, with an initial diameter of 7.02 mm, is in an oven at 923 K with an ambient of 0.125 oxygen mole fraction. The sequence of images is: (a) initial droplet (b) drying stage (c) start of devolatilization and (d) maximum swollen volume. The white areas behind the droplet are the glowing hot coils of the oven. The test maximum swollen volume occurs a few seconds after the reduced-gravity period ended (during the pull-up).
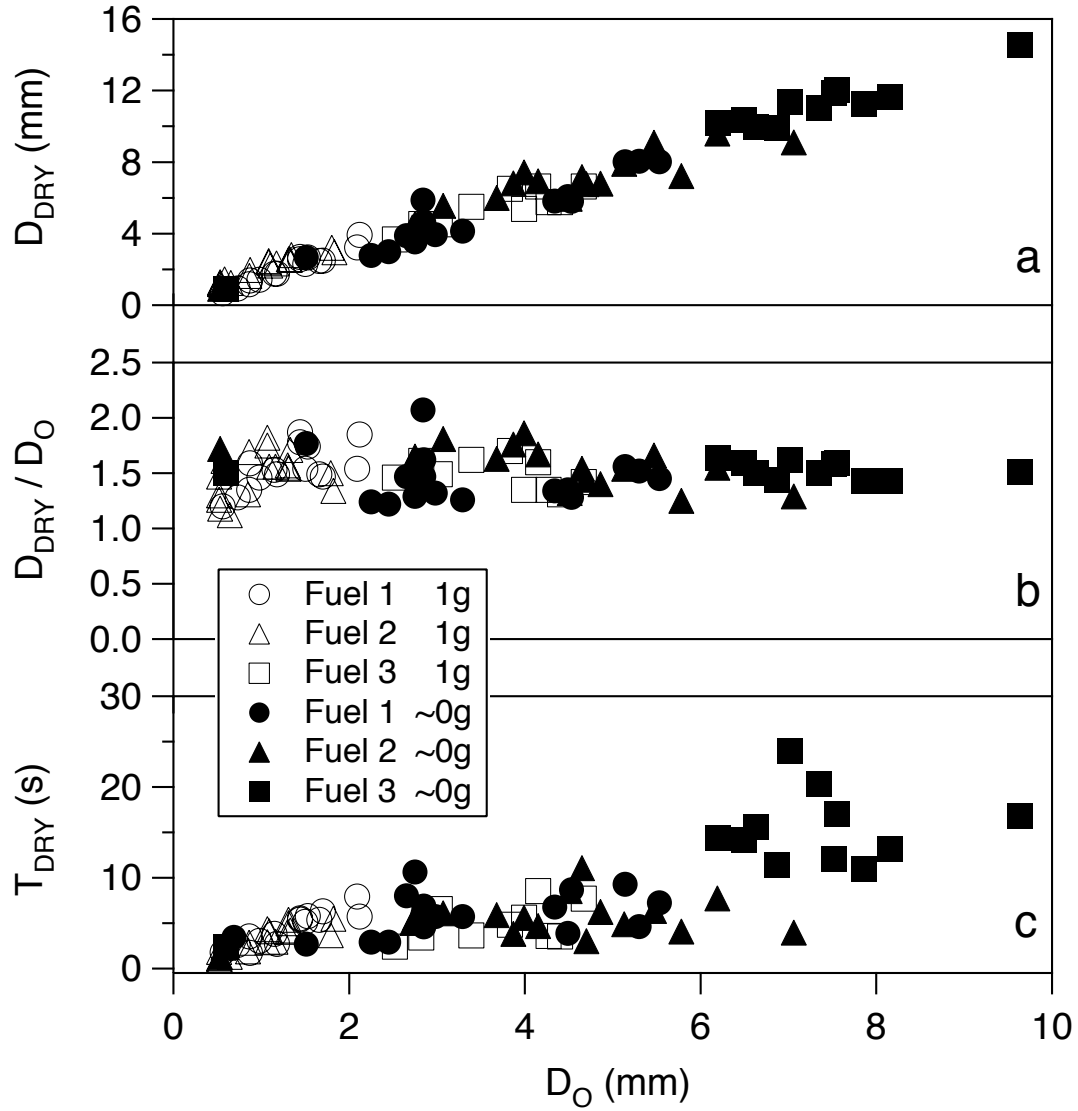
Fig. 4. (a) Drying diameter versus initial diameter, (b) drying diameter normalized against its initial diameter versus initial diameter and (c) drying time versus initial diameter for tests conducted at 923 K where the oxygen mole fraction varies from 0.0 to 0.21.
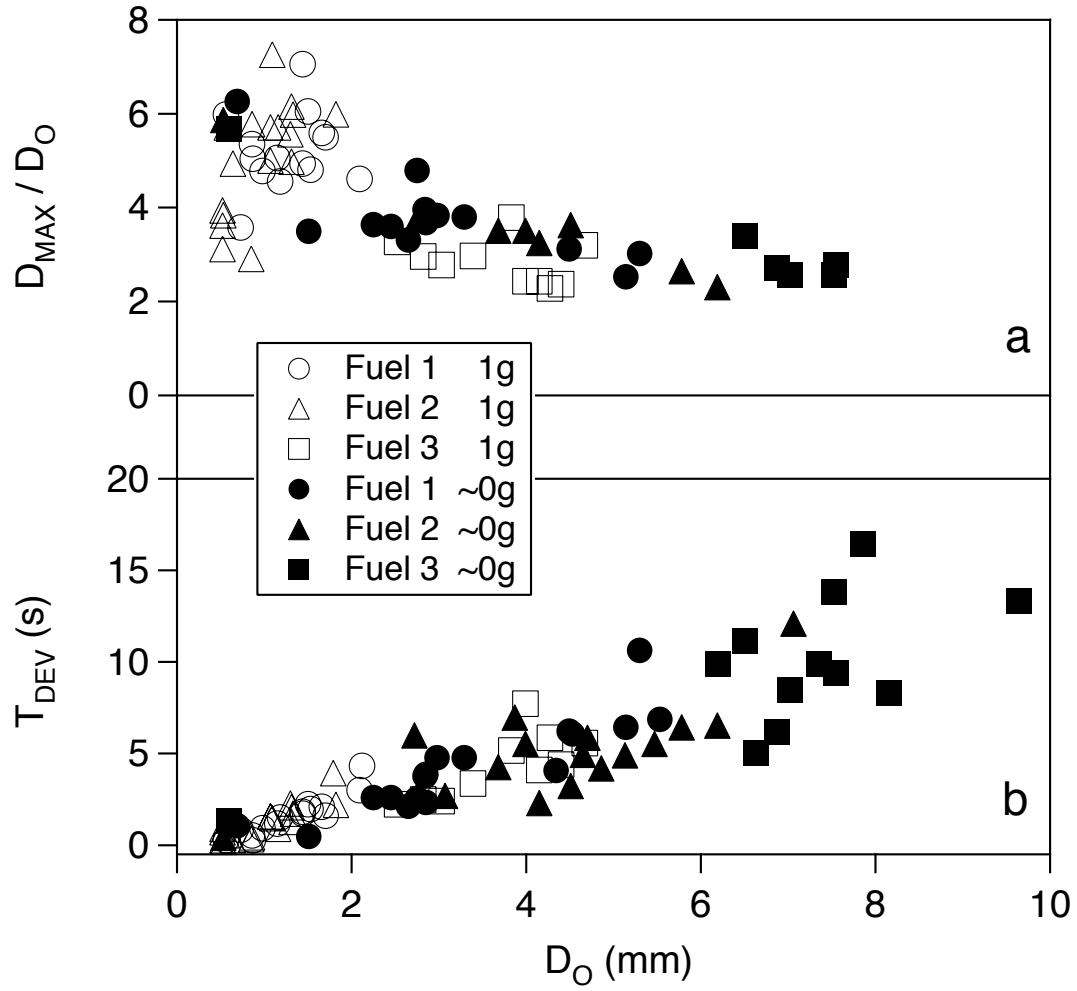
Fig. 5. (a) Maximum diameter normalized against its initial diameter versus initial diameter and (b) devolatilization time versus initial diameter for tests conducted at 923 K where the oxygen mole fraction varies from 0.0 to 0.21.

Table 1
Tabulation of sphericity data at each stage for four test groups. Within each group, only the oxygen mole fraction varies. The four groups of test conditions are: (a) Fuel 1, Normal Gravity, $D_O = 1.51\,mm$, (b) Fuel 1, Reduced Gravity, $D_O = 2.83\,mm$, (c) Fuel 3, Normal Gravity, $D_O = 4.41\,mm$ and (d) Fuel 2, Reduced Gravity, $D_O = 4.69\,mm$. All tests had an oven temperature of $923\,K$.

X_{O2}	S_O	S_{DRY}	S_{MAX}	S_{CHAR}	S_{SHRINK}	Test Type
(a) Fuel 1, Normal Gravity, $D_0 = 1.51\,mm \pm 0.09\,mm$						
0.0	0.99	0.98	0.95	-	0.96	Pyrolysis
0.025	0.97	0.91	0.81	-	0.82	Pyrolysis
0.05	0.98	0.95	0.70	-	0.72	Pyrolysis
0.075	0.98	0.89	0.80	-	-	Pyrolysis
0.21	0.98	0.89	0.64	0.97	-	Complete Combustion
(b) Fuel 1, Reduced Gravity, $D_0 = 2.83\,mm \pm 0.14\,mm$						
0.0	0.79	0.85	0.90	-	0.91	Pyrolysis
0.075	0.83	0.89	0.84	-	-	Pyrolysis
0.10	0.95	0.92	0.84	0.85	-	Partial Combustion
0.15	0.79	0.92	0.78	0.75	-	Partial Combustion
(c) Fuel 3, Normal Gravity, $D_0 = 4.41\,mm \pm 0.19\,mm$						
0.0	0.96	0.85	0.92	-	0.89	Pyrolysis
0.15	0.91	0.94	0.85	-	-	Pyrolysis
0.21	0.95	0.87	0.79	0.98	-	Complete Combustion
(d) Fuel 2, Reduced Gravity, $D_0 = 4.69\,mm \pm 0.18\,mm$						
0.0	0.71	0.86	0.87	-	-	Pyrolysis
0.10	0.96	0.89	0.71	0.72	-	Partial Combustion
0.175	0.85	0.91	n/a	n/a	-	Incomplete Combustion